

Investigation of Various Microwave Electron Cyclotron Resonance Cathode Configurations

IEPC-2005-283

Presented at the 29th International Electric Propulsion Conference, Princeton University,
October 31 – November 4, 2005

Hani Kamhawi* and John E. Foster.†
NASA Glenn Research Center, Cleveland, Ohio 44135

Abstract: Progress has been made on the investigation of various electron cyclotron resonance (ECR) cathode configurations. The operation of a high-current ECR cathode was successfully demonstrated at 2.45 and 5.85 GHz. At 2.45 GHz and 100 W of input μ wave power, a configuration utilizing a longitudinal antenna attained an electron extraction current of 2.6 A at a xenon flow rate of 3 sccm and an extraction voltage of 60 V. Whereas, at 5.85 GHz and 100 W of input μ wave power, a longitudinal antenna configuration achieved an electron extraction current of 2.5 A at a xenon flow rate of 8 sccm and an extraction voltage of 60 V. Also, a multi-slotted ECR cathode was successfully operated at 5.85 GHz and 100 W of input μ wave power and demonstrated an electron extraction current of 1.73 A at a xenon flow rate of 4 sccm and an extraction voltage of 90 V.

Nomenclature

| | |
|------------------|---|
| A | = Amperes |
| B | = Magnetic field strength, G |
| B _{res} | = Resonance magnetic field strength, G |
| cm | = Centimeter |
| e | = Electron charge, 1.602×10^{-19} C |
| f _p | = Plasma frequency, Hz |
| G | = Gauss |
| GHz | = Giga hertz |
| h | = Hour |
| k | = Boltzmann constant, 1.38×10^{-23} J/K |
| kg | = Kilogram |
| m | = Milli |
| m _e | = Electron mass, 9.11×10^{-31} kg |
| M _i | = Ion mass, kg |
| n _e | = Electron number density, cm ⁻³ |
| rf | = Radio frequency |
| s | = Seconds |
| Sccm | = Standard cubic centimeters per minute |
| Sm-co | = Samarium cobalt |
| T _e | = Electron temperature, eV |
| W | = Watts |
| ϵ_0 | = permittivity of free space, 8.854×10^{-12} F/m |
| Γ_i | = Ion current density, A/m ² |
| ω_p | = Plasma frequency, radians/s |
| ω_μ | = μ wave excitation frequency, radians/s |
| ω_{ce} | = Electron cyclotron frequency, radians/s |

* Research Engineer, Electric Propulsion Branch, Hani.kamhawi-1@nasa.gov.

† Research Engineer, Electric Propulsion Branch, John.E.Foster@nasa.gov.

I. Introduction

Propulsion systems capable of providing very high specific impulse (6000-9000 s) are desirable for long-term missions to the outer planets and beyond.^{1,2,3} State-of-the-art ion thruster system technology satisfies the high specific impulse requirement; however, the lifetime of these thruster systems has only been demonstrated for up to ~30,000 hrs which is far below the required operational lifetime of 7-14 years required for travel to the outer planets and beyond. Such long, continuous operation times place extraordinary lifetime requirements on thruster components and subsystems.^{4,5,6,7} This implies that ion thruster operation lifetime has to extend well above the state-of-the-art to accomplish long-duration missions. In general, ion thruster lifetime is limited by four potential failure modes: 1.) discharge cathode failure, 2.) neutralizer cathode failure, 3.) ion optics failure and 4.) electron back-streaming failure. Failure of either the discharge or neutralizer cathodes is related primarily to hollow cathode failure mechanisms. Hollow cathode main failure mechanisms include depletion of the emitter impregnate, physical sputter damage due to exposure to ion bombardment from both ambient discharge plasma ions and locally produced energetic ions, and physical process occurring at emitter surface inhibiting emitter thermionic emission properties.⁸ Researchers expect that hollow cathode lifetime will be the limiting factor for extended-duration operation in both ion propulsion systems and hall thrusters once grid erosion and thruster channel erosion are respectively mitigated.

The focus of this paper is the elimination of the hollow cathode failure modes. Recently, NASA Glenn Research Center (GRC) received a NRA award to develop an electrode-less cathode for charge neutralization under the support of Prometheus Nuclear Systems and Technologies Advanced Systems and Technology Project Office. The goal of the multi-year effort is to eliminate the lifetime issues associated with conventional hollow cathodes by investigating electrode-less plasma production approaches. An electron cyclotron resonance (ECR) discharge is proposed as an alternative to hollow cathodes for plasma generation. ECR discharges offer a number of distinct advantages over hollow cathode:^{9,10,11,12,13}

- Lifetime of μ wave discharge plasma production is mostly limited by the life of the power tube, which have typically demonstrated lifetimes in excess of 10 years.
- μ wave power generation tubes have efficiencies as high as 90%.
- High purity xenon is not a requirement which results in substantial cost savings.
- ECR discharges operate at lower plasma potentials resulting in lower sputter erosion rates of the propulsion system.

ECR ion sources are widely used in material processing applications, different types of accelerator for nuclear research, ion milling and implantation, and mass spectrometers among other applications.^{14,15,16,17} Investigation of μ wave based ion thrusters at NASA GRC dates back to the 1980s.¹⁸ The Japanese have maintained a vibrant microwave ion thruster and development effort dating back to the late 1980s to the present. Researchers in Japan investigated and demonstrated the use of ECR cathodes for beam neutralization. Several ECR cathode assemblies were developed at μ wave frequencies of 4.2 GHz.¹⁹⁻²⁴ They demonstrated electron neutralization currents up to 0.5 A at μ wave input power of approximately 20 W for xenon flow rates of 1 sccm.²¹ Additionally, researchers in Japan performed an 18,000 h endurance test for a μ wave discharge ion thruster engineering model that employed an ECR neutralizer.²² Their work culminated in the launch of a space science mission to an asteroid using ion propulsion.²⁵

II. Background

Main discharge plasma production and neutralizer applications both have the potential to use electrode-less plasma cathodes rather than conventional hollow cathodes. Parametric analysis, including considerations of power requirements, ease of implementation, simplicity, internal neutral pressure operating range, and maximum achievable plasma density, revealed that the μ wave ECR discharge approach was the most appropriate plasma generation method of the potential rf schemes.¹⁰

The ECR cathode belongs to a general family of electron sources known as plasma cathodes. The source electrons from a plasma cathode are those extracted from a sheath at the boundary of dense plasma. Unlike conventional hot filament or hollow cathode sources, the source of electrons is the plasma itself, and contributions due to field emission and thermionic emission are typically negligible.²⁶ In ECR cathodes, the equilibrium loss rate of electrons must equal that of the ions; therefore, the emitted electron current must equal the ion current collected at the chamber walls. Ions are lost to the boundaries at the Bohm speed, with an ion flux rate of¹⁷

$$\Gamma_i = 0.61en\sqrt{\frac{kT_e}{M_i}} \quad (1)$$

In an ECR discharge, the source of energy for plasma generation and maintenance is ECR heating of the plasma electrons with μ wave radiation. Electron number density and temperature, and electron energy population distribution characterize ECR source performance. In an ECR source, electrons resonantly absorb μ wave radiation at the electron cyclotron frequency determined by the local magnetic field. Whenever the μ wave frequency is tuned to the electron-cyclotron-frequency, electrons can be resonantly excited and thereby given sufficient energy to cause ionization within a low pressure gas, additionally, at low collision frequency some of the electrons are coherently excited and given high energies which can generate multiply charged ions.²⁶ In an ECR source, the magnetic field is generated by permanent or electro-magnets. The resonant absorption occurs when and where the input μ wave frequency equals the electron cyclotron frequency as given by

$$\omega_\mu = \omega_{ce}, \quad \omega_{ce} = \frac{eB}{m_e} \quad (2)$$

Figure 1 presents a plot of the required magnetic field strength necessary to achieve resonance for μ wave frequencies up to 7 GHz. For this effort, two different μ wave frequencies were investigated: 2.45 and 5.8 GHz. At 2.45 GHz, the resonant process takes place at contour surfaces of constant magnetic field strength (B_{res}) of approximately 875 G. At 5.8 GHz, the resonant absorption takes place at contour surfaces of constant magnetic field strength of approximately 2100 G. In general, the hot electrons produced during this process ionize neutral gas, thereby generating the discharge plasma completely electrode-lessly.

The maximum value of the emitted electron flux rate is equal to the ion flux rate; thus, electron current from the ECR cathode is determined by the flow of ions to the walls. To maximize the electron flux, one attempts to maximize the plasma density. An estimate of the cut-off plasma density in an ECR cathode is obtained by equating the μ wave frequency to the plasma frequency as given by

$$\omega_p = \left(\frac{n_e e^2}{\epsilon_0 m_e} \right)^{1/2}, \quad f_p = \frac{\omega_p}{2\pi} \quad (3)$$

Microwave frequencies below the plasma frequency do not propagate. Instead, there is only evanescent penetration so that heating takes place within of order $\frac{1}{2}$ a wavelength from the μ wave source. Low density operation can be avoided by operating at a higher μ wave frequency, hence this is the basis for investigating the 5.8 GHz frequency in addition to the 2.45 GHz frequency. By equating equations 1 and 3, the maximum plasma density for μ wave propagation and absorption is found. Figure 1 presents the cut-off plasma density magnitudes for the different operating μ wave frequencies. At 2.45 GHz the cut-off density magnitude is $7.5 \times 10^{10} \text{ cm}^{-3}$ while at 5.8 GHz it is $4.3 \times 10^{11} \text{ cm}^{-3}$. Based on cut-off considerations, the maximum plasma density generally increases with the square of the μ wave frequency. In practice, plasma densities above this cut-off limit are achievable, and heating occurs by the evanescent penetration of the μ wave s into the heating zones.

The work presented here is a continuation of earlier ECR cathode work at NASA GRC.^{27,28} The goal of this and future efforts is to develop an ECR cathode that is capable of supplying electron neutralization currents from 3 to 5 A and that can be implemented and integrated into an ion propulsion systems.¹⁰ Improvements in the ECR cathode design have been implemented and a summary of the recent results at 2.45 and 5.8 GHz will be reported here.

III. Test Support Hardware

This section provides a brief description of the test support hardware employed in the ECR cathode testing, including the 2.45 and 5.8 GHz μ wave power generators, the gas feed system, and the vacuum facility utilized in testing.

A. 2.45 and 5.8 GHz Microwave Power Generators

Microwave power generators operating at 2.45 and 5.8 GHz were used in this effort. The 2.45 GHz source is a variable power output, air-cooled unit capable of outputting between 0 and 300 W. The power supply contains detectors to measure forward and reflected power at the power supply. A water-cooled isolator attached to the output of the generator protects the unit from excessive reflected power. Microwave power is fed into the vacuum chamber by a specially fabricated flange that permits the μ wave coaxial cable to be fed thru to the inside of the vacuum

chamber. Figure 2 shows the 2.45 GHz source with the water cooled circulator and coaxial μ wave power cable and the associated vacuum flange.

The 5.8 GHz source is a completely integrated system designed for high-performance delivery of μ wave power up to 700 W. The unit is air-cooled but provisions for water cooling are available for cases when 1000 W of continuous power is required. The waveguide in this configuration was WR159. Figures 3 and 4 show the 5.8 GHz μ wave circuit for the different antenna configurations that were tested. For both circuits, the 5.8 GHz magnetron output is attached to a 1300 W 3-port circulator that channels the reflected power to a convectively cooled dummy load. A -60 dB two port directional coupler is attached to the output of port 3 and to two μ wave power meters that measure and display the forward and reflected power. A 4-stub tuner was attached to the downstream end of the directional coupler output to provide impedance matching of the transmitted power to the plasma load, thus minimizing reflected power and maximizing power into the plasma. When testing the longitudinal antenna ECR cathode, a waveguide to coaxial adaptor (end launcher) connected to the 4-stub tuner converted the μ wave output from waveguide to coaxial line so that it would be compatible with the high-power water-cooled μ wave coaxial cable. However, when testing the single slot and multi-slot ECR cathodes, the μ wave power was fed into the vacuum chamber via an alumina μ wave window that also served as a vacuum seal. Prior to testing with the ECR neutralizer, both μ wave sources (2.45 and 5.85 GHz) along with their various components were operated with a dummy load placed at the end of the μ wave transmission line to confirm power transmission.

B. Vacuum Facility

Tests were conducted in Vacuum Facility 11 (VF-11). VF-11 is a cryopumped facility, 2.5 m in diameter and 8 m long. Three 48" cryotubs and four 24" cryopumps provide 100,000 L/s pumping speed on xenon and produce a base pressure of 2×10^{-7} Torr. The facility has two isolated test ports. Tests were conducted in Port 3 as shown in Figure 5. Port 3 is 0.3 m in diameter and is 0.65 m long and can be independently evacuated via cryopump. Port 3 is isolated from the main vacuum chamber via a gate valve. Port 3 propellant feed system consists of two mass flow controllers: 10 and 20 sccm. A 750 W (2.5 A 300 V) laboratory power supply was used to provide the bias voltage for electron current extraction.

Port 3 can either be evacuated by opening the gate valve isolating Port 3 from VF-11 or by using Port 3 cryopump. VF-11 has a typical base pressure of 2×10^{-7} Torr which results in a Port 3 base pressure of 2×10^{-6} Torr. During testing, operating pressure base ranged from 7.8×10^{-5} Torr at 5 sccm to 2.0×10^{-4} Torr at 10 sccm of xenon flow.

IV. Test Article

The laboratory ECR cathodes used in this study were fabricated from mild steel. No exotic materials were used since the goals of this experiment were to perform a preliminary evaluation of different design variations so as to eventually arrive at an optimum design. For this study a number of ECR cathode configurations were tested and include:

1. Configurations 1a and 1b: Cylindrical chamber ECR cathode(s) with μ wave power launched via a longitudinal antenna
2. Configuration 2: A rectangular chamber ECR cathode with single-slot antenna for μ wave injection
3. Configuration 3a and 3b: A rectangular chamber ECR cathode with multi-slots for μ wave injection²⁹

The main components of the cylindrical ECR cathode are: the coaxial μ wave adaptor that feeds the μ wave power into the longitudinal antenna, the propellant injection feed lines, the extraction slot, magnetic circuit, and the cylindrical ECR cathode discharge chamber. Samarium cobalt (Sm-Co) permanent magnet rings provided the magnetic field strength necessary to achieve ECR.

For the single slot ECR cathode, an adaptor plate was attached to the end of the WR159 waveguide vacuum flange and mounted to it was the ECR cathode which contained the propellant feed ports and magnetic circuit. The multi-slot ECR cathode injected μ waves into the ECR discharge chamber (which consists of 4 side walls attached to a WR159 waveguide) via a slotted antenna, a waveguide structure that contains radiating, periodically spaced slots; the slotted antenna was designed such that μ wave power is distributed evenly to each slot.²⁹ A positively biased molybdenum electrode was placed approximately 3 cm downstream of the ECR cathode exit plane to collect the electron current and the ECR cathode chamber assembly was at ground potential.

V. Results and Discussion

Previous studies have shown that ECR neutralizers are sensitive to a number of parameters.^{27,28} This study evaluated the performance of various ECR cathode configurations that incorporate the implementation of different antennas for launching and injecting μ wave power into the ECR chamber. Additionally, evaluation of the effect of varying the propellant flow rate, and magnetic field strength (i.e, magnetic circuit) inside the ECR cathode on the magnitude of the electron extraction current was performed. In this section, results will first be presented for ECR cathode operation at 2.45 GHz where a longitudinal antenna was used to launch the μ wave power into a cylindrical ECR cathode chamber. Next, results will be presented for ECR cathode operation at 5.85 GHz for three distinctly different ECR cathode chamber configurations that utilize different antenna types to launch the μ wave power into the ECR cathode chamber.

A. 2.45 GHz

Testing of the longitudinal antenna ECR cathode was performed using two cylindrical ECR cathode discharge chambers. Configuration 1a was reported last year and Configuration 1b is a new design with a different aspect ratio when compared to Configuration 1a.²⁸ For Configuration 1a, a different magnetic circuit and extraction slot opening geometry (when compared to previous work²⁸) were implemented to improve the ECR discharge performance at 2.45 GHz. Several variations of the magnetic circuit were investigated; this report presents the results for the magnetic circuit and slot opening geometry that attained the highest performance. Configuration 1b implemented the same magnetic circuit and slot opening geometry that was used in Configuration 1a, however, the chamber volume was varied. For both configurations, tests were performed to extract an electron current at extraction voltages between 30 and 60 V and μ wave input power of 75 W and 100 W. The xenon propellant flow rate was varied between 2 and 10 sccm.

1. Configuration 1a

Configuration 1a uses the same discharge chamber that was reported earlier, however, the magnetic circuit (magnetic field strength and shape) and extraction slot location and opening size were further optimized. A number of variations were tested and results presented in this report will present the results from the best performing magnetic circuit and slot configurations.

Figure 6 shows the ECR cathode operating during current extraction at 100 W. Figures 7 and 8 present plots of the variation in electron extraction current for a range of extraction voltages at varying xenon propellant flow rates for μ wave input power of 75 and 100 W, respectively. In general, results in Figs. 7 and 8 indicate that increasing the propellant flow rate increased the magnitude of the extracted current for a given extraction voltage at a specific μ wave input power. For example, at an extraction voltage of 45 V and μ wave input power of 100 W, the electron extraction current was 0.93, 1.4, and 1.45 A for xenon flow rates of 5, 7.5, and 10 sccm, respectively. Results presented in Fig. 7 for extraction voltage above 45 V are not reliable since a pressure spike occurred in the facility base pressure when the data was collected and caused the anomalous results. In general results in Figs. 7 and 8 indicate that increasing the xenon flow rate results in a higher internal pressure inside the ECR discharge chamber which reduces the mean free path and increases the collision frequency, thus resulting in higher ionization rates. Additionally, results in Figs. 7 and 8 indicate that increasing the magnitude of input μ wave power increases the magnitude of the extracted electron current at a given extraction voltage and propellant flow rate. For example, at an extraction voltage of 60 V and xenon flow rate of 5 sccm, the extraction current magnitude is 1.4 and 1.6 A for μ wave input power of 75 and 100 W, respectively. Higher μ wave input power, at given test conditions, result in higher electron extraction currents due likely to increases in electron number densities which approach the cut-off density (Eq. 3).

Figure 9 presents the variation in the electron extraction current as the xenon propellant flow rate is varied from 2 to 10 sccm at extraction voltage magnitudes of 45 and 60 V for μ wave input power of 100 W. Results in Fig. 9 indicate that for a given extraction voltage increasing the xenon propellant flow rate results in a monotonic growth of the electron extraction current which reaches a maximum at 8 sccm, this might be an indication that once the cut-off density is attained and additional propellant is introduced into the ECR zone, disruptions to the ECR energy transfer occur resulting in no additional gain or reduction to the electron extraction current. Results in Fig. 9 indicate that a maximum electron extraction current of 2.5 A is achieved for a xenon propellant flow rate of 9 sccm at an extraction voltage of 60 V at 100 W of input μ wave power. Also, Fig. 9 indicates that at an extraction voltage of 45 V, the maximum extraction current achieved is 1.38 A at a xenon propellant flow rate of 9 sccm for 100 W of input μ wave power. Hence increasing the extraction voltage results in the energetic electrons escaping from the extraction sheath and due to their higher energies contribute additional ionization in the plume area.

2. Configuration 1b

Configuration 1b employed the same optimized magnetic circuit and slot geometry as Configuration 1a, however, the ECR discharge chamber had a different aspect ratio (length to diameter ratio). Figures 10 and 11 present plots of the variation in the electron extraction current for a range of extraction voltages at varying xenon propellant flow rates for μ wave input power of 75 and 100 W, respectively. In general, results in Figs. 10 and 11 indicate that increasing the propellant flow rate increased the magnitude of the extracted current for a given extraction voltage at a specific μ wave input power as was observed for Configuration 1a. For example, at an extraction voltage of 45 V and μ wave input power of 100 W, the electron extraction current was 1.24, 1.38, and 1.44 A for xenon flow rates of 5, 7.5, and 10 sccm, respectively. Additionally, results in Figs. 10 and 11 indicate that increasing the magnitude of input μ wave power increases the magnitude of the extracted electron current at a given extraction voltage magnitude and propellant flow rate as has been observed for Configuration 1a. For example, at an extraction voltage of 60 V and xenon flow rate of 5 sccm, the extraction current magnitude is 2.07 and > 2.63 A (the maximum current the power supply can provide) for μ wave input power of 75 and 100 W, respectively.

Figure 12 presents the variation in the electron extraction current as the xenon propellant flow rate is varied from 2 to 10 sccm at extraction voltage magnitudes of 45, 50, 55 and 60 V for μ wave input power of 100 W. Results in Fig. 12 indicate that as the extraction voltage magnitude is increased from 45 to 60 V, the variation of electron extraction current magnitude with the varying propellant flow rate becomes flatter. Results in Fig. 12 indicate that maximum electron extraction current of 2.63 A (maximum current power supply can provide) is achieved for a xenon propellant flow rate of 3 sccm at an extraction voltage of 60 V at 100 W of input μ wave power.

Comparison of results presented for Configurations 1a and 1b indicates that Configuration 1b performance exceeds that of Configuration 1a. For a given input μ wave power at a given propellant flow rate and extraction voltage, Configuration 1b will supply exceedingly higher electron extraction currents. Additionally, For Configuration 1b, it is observed that the electron extraction current magnitudes at a given extraction voltage are closer in value than their counterparts in Configuration 1a, this is mainly attributed to the reduced ECR cathode discharge chamber volume of Configuration 1b when compared to 1a which results in a higher internal pressure for a given flow rate, thus smaller mean free paths and higher collision frequencies and ionization rates.

B. 5.85 GHz

Three different ECR cathode geometries were tested at a μ wave frequency of 5.85 GHz: Configurations 1a, 2, and 3. Configuration 1a is the same configuration that was tested at 2.45 GHz, Configuration 2 is a single slot ECR cathode, and Configuration 3 is the multi-slot rectangular ECR cathode.

1. Configuration 1a

Tests of Configurations 1a were also performed at μ wave input frequency of 5.85 GHz. Figure 13 presents the variation in electron extraction current for a range of extraction voltages at varying xenon propellant flow rates for μ wave input power of 100 W. In general, results in Fig. 13 indicate that increasing the propellant flow rate increased the magnitude of the extracted current for a given extraction voltage at a specific μ wave input power. For example, at an extraction voltage of 45 V, the electron extraction current was 0.65, 1.26, and 1.42 A for xenon flow rates of 5, 7.5, and 10 sccm, respectively.

Figure 14 presents the variation in the electron extraction current as the xenon propellant flow rate is varied from 2 to 10 sccm at extraction voltage magnitudes of 45 and 60 V for μ wave input power of 100 W. Results in Fig. 14 indicate (as was measured during 2.45 GHz testing) that a maximum electron extraction current of 2.4 A is achieved for a xenon propellant flow rate of 8 sccm at an extraction voltage of 60 V at 100 W of input μ wave power. Additionally, Fig. 14 indicates that at an extraction voltage of 45 V, the maximum extraction current achieved is 1.52 A at a xenon propellant flow rate of 10 sccm.

Comparing results from 2.45 and 5.85 GHz operation for Configuration 1a indicates that the performance at the two different μ wave frequencies was very comparable and that no substantial gains in extraction current magnitudes (specially at the lower propellant flow rates) were gained due to operation at higher μ wave frequencies. This might indicate that overdense plasma production ($\omega_p > \omega_\mu$) is taking place while operating at 2.45 GHz. Additionally, ECR discharge initiation at 2.45 GHz was instantaneous for operation at 2.45 GHz, whereas, to initiate the ECR discharge at 5.85 GHz the extraction voltage magnitude was set to ~ 100 V and once the ECR discharge was “turned on” the extraction voltage magnitude was lowered and data was collected.

Finally, it is important to note that unsuccessful attempts were made to test Configuration 1b at 5.85 GHz. Although an ECR discharge was sporadically achieved, attempts to sustain and reignite the discharge were mostly unsuccessful.

2. Configuration 2

Configuration 2 employed a single slot to launch and inject μ wave power into the rectangular ECR discharge chamber. In this paper, only a summary of the performance will be presented since, ultimately, this configuration performance failed to meet the electron extraction current requirements.

Configuration 2 was tested at μ wave input power ranging from 20 to 100 W and extraction voltage magnitudes ranging from 45 to 140 V. Several variations of the magnetic circuit were evaluated before arriving at the magnetic circuit that provided the best performance. Tests of Configuration 2 revealed that at 45 W of input power and a xenon flow rate of 2.6 sccm the maximum electron extraction current achieved was 0.64 A at an extraction voltage of 110 V. Additionally, at 45 W of input power and a xenon flow rate of 2.6 sccm the maximum electron extraction current achieved was 0.05 A at an extraction voltage of 45 V. Utilizing the same configuration and testing at 20 W of input μ wave power and a xenon flow rate of 4 sccm an extraction current of 0.15 A was achieved at an extraction voltage of 45 V. It was also observed that increasing the magnitude of input μ wave power did not result in increased electron extraction current magnitudes and in some cases reduced such magnitudes.

3. Configuration 3

Testing of the multi-slot ECR cathode was performed at μ wave input power of 75, 100, and 150 W. Xenon propellant flow rates were varied between 2 and 7 sccm. Extraction voltage magnitudes were 45, 65, and 90 V. The results presented in this section present performance results after several iterations on the ECR cathode magnetic circuit. Two variations on the bias plate location were tested. In the first setup, Configuration 3a, the bias plate was mounted at the ECR cathode end plane and was electrically isolated from the ECR cathode via 1.25 cm long high voltage insulators. In the second setup, Configuration 3b, there was no end plate and the molybdenum bias plate was placed 3 cm away from the ECR cathode end plane.

a. Configuration 3a

For Configuration 3a, Fig. 15 presents the electron extraction current magnitudes for μ wave input power of 100 W for extraction voltage magnitudes of 45, 65, and 90 V. At an extraction voltage of 45 V a maximum electron extraction current of 0.81 A was achieved at a xenon propellant flow rate of 4.46 sccm. At an extraction voltage of 65 V a maximum electron extraction current of 1.24 A was achieved at a xenon propellant flow rate of 3.75 sccm. Finally, at an extraction voltage of 90 V a maximum electron extraction current of 1.73 A was achieved at a xenon propellant flow rate of 4 sccm. Results in Fig. 15 indicate that as the xenon flow rate was increased, the electron extraction current magnitude increased and reached a maximum, subsequent increases in the xenon flow rate greatly reduced the electron extraction current magnitude. It is speculated that as additional xenon is injected, the electron-neutral collision frequency increased which resulted in a loss in the high-energy tail electron population. Additionally, Configuration 3a was operated at 75 and 150 W. At 75 W, the maximum electron extraction current magnitude was: 0.77 A at 45 V with a xenon flow rate of 4.7 sccm, 1.17 A at 65 V with a xenon flow rate of 4.1 sccm, 1.53 A at 90 V with a xenon flow rate of 3.7 sccm. At 150 W, the maximum electron extraction current magnitude was: 0.86 A at 45 V with a xenon flow rate of 4.92 sccm, 1.44 A at 65 V with a xenon flow rate of 4.4 sccm, 1.92 A at 90 V with a xenon flow rate of 4.26 sccm. Hence, doubling the μ wave power only increased the electron extraction current magnitude by $\sim 25\%$ at 90 V. This indicates that the coupling efficiency at higher μ wave powers is not as effective as at the lower power which might be due to the fact that an overdense plasma exists at the antenna slots.

b. Configuration 3b

For Configuration 3b, Fig. 16 presents the electron extraction current magnitudes for μ wave input power of 100 W for extraction voltage magnitudes of 45, 65, and 90 V. At an extraction voltage of 45 V a maximum electron extraction current of 0.3 A was achieved at a xenon propellant flow rate of 4 sccm. At an extraction voltage of 65 V a maximum electron extraction current of 1 A was achieved at a xenon propellant flow rate of 5.64 sccm. Finally, at an extraction voltage of 90 V a maximum electron extraction current of 1.38 A was achieved at a xenon propellant flow rate of 5.3 sccm. Additionally, Configuration 3b was operated at 75 and 150 W. At 75 W, the maximum electron extraction current magnitude was: 0.28 A at 45 V with a xenon flow rate of 6.23 sccm, 0.74 A at 65 V with a xenon flow rate of 5.74 sccm, and 1.07 A at 90 V with a xenon flow rate of 5.3 sccm. At 150 W, the maximum electron extraction current magnitude was: 0.32 A at 45 V with a xenon flow rate of 4.53 sccm, 1.2 A at 65 V with a xenon flow rate of 5.78 sccm, 1.67 A at 90 V with a xenon flow rate of 5.38 sccm.

Electron extraction current magnitudes for Configuration 3a exceed Configuration 3b magnitudes and the peak electron extraction current magnitudes for Configuration 1a occur at lower xenon flow rates indicating more efficient propellant utilization. This is mainly attributed to placing the bias plate at the ECR cathode end plane which

results in reduced neutral flow out of the device leading to higher internal pressure (due to neutrals drifting and reflecting of end plate). Additionally, penetrating μ waves reflect off the end wall and reflect back into the discharge chamber and cause additional ECR ionization and higher electron extraction currents.

VI. Conclusions

The operation of a high-current ECR cathode was successfully demonstrated at 2.45 and 5.85 GHz. At 2.45 GHz and 100 W of input μ wave power, a configuration utilizing a longitudinal antenna attained an electron extraction current of 2.6 A for a xenon flow rate of 3 sccm at an extraction voltage of 60 V. At 5.85 GHz and 100 W of input μ wave power, a configuration utilizing a longitudinal antenna achieved 2.5 A electron extraction current for a xenon flow rate of 8 sccm at an extraction voltage of 60 V. Also, a multi-slotted ECR cathode was successfully operated at 5.85 GHz and supplied an electron extraction current of 1.77 A at 90 V.

Additional design optimization will be performed for Configurations 1a and 3a to improve their performance and to better assess which design is more suitable for long duration operation. To attain a better understanding of the details of the both ECR cathode operation, which will assist in the design optimization, detailed plasma properties inside the ECR discharge and in the plume area have to be performed and will include electron temperature, number density, plasma potential, and charge state composition using emission spectroscopy.

Acknowledgments

This work has been supported under a NRA award to develop an electrode-less cathode for charge neutralization under the support of Prometheus Nuclear Systems and Technologies Advanced Systems and Technology Project Office.

References

- ¹Oleson, S.R., "Electric Propulsion for Project Prometheus," 39th Joint Propulsion Conference, July, 2003, Huntsville, Al, AIAA-2003-5279.
- ²Oleson, S.R., *et al*, "Outer Planet Exploration with Advanced Radioisotope Electric Propulsion," 27th International Electric Propulsion Conference, Oct. 2001, Pasadena, CA, IEPC-01-0179.
- ³Oleson, S., "Electric Propulsion Technology Development for the Jupiter Icy Moon Orbiter Project," Proceedings of the 40th Joint Propulsion Conference, AIAA Paper 2004-3449, July 2004.
- ⁴Rawlin, *et al*, "High Specific Impulse High Power Ion Engine Operation," AIAA Paper 2002-3838, July 2002.
- ⁵Rawlin, V. K., *et al*, "An Ion Propulsion Systems for NASA's Deep Space Missions," AIAA 1999-4612.
- ⁶Polk, J.E., *et al*, "In-Flight Performance of the NSTAR Ion Propulsion System on the Deep Space One Mission," IEEE Aerospace Conference Paper 8.0304, March 2000.
- ⁷Sengupta, A., *et al*, "Status of The Extended Life Test of the Deep Space 1 Flight Spare Ion Engine after 30,352 Hours of Operation," AIAA-2003-4558.
- ⁸Sarver-Verhey, T.R., "Scenerio for Hollow Cathode End of Life," International Electric Propulsion Conference, Pasadena, October 2001, IEPC paper 01-270.
- ⁹Foster, J.E. and Patterson, M.J., "Status of Microwave Thruster Development Activity at NASA GRC," AIAA Paper 2002 - 3837.
- ¹⁰Foster, J.E., *et al*, "The High Power Electric Propulsion (HiPEP) Ion Thruster," AIAA 2004-3812.
- ¹¹Foster, J.E., Kamhawi, H., Haag, T., Williams, G., and Carpenter, C., "High Power ECR Ion Thruster Discharge Characterization," IEPC-2005-272.
- ¹²Bering, E.A., Chang-Diaz, F., and Squire, J., "The Use of RF waves for Space Propulsion Systems," *The Radio Science Bulletin*, No. 310, September 2004, pp. 92-106.
- ¹³Roth, R., Industrial Plasma Engineering: Volume I, Institute of Physics Publishing, 2001.
- ¹⁴Geller, R., *Electron Cyclotron Resonance Ion Sources and ECR Plasmas*, Institute of Physics Publishing, Bristol and Philadelphia, 1996.
- ¹⁵Lieberman, M. A., and Lichtenberg, A. J., "Principles of Plasma Discharges and Materials Processing," John and Wiley, 1994.
- ¹⁶Zhang, H., Ion Sources, Science Press, 1999.

- ¹⁷Chen, F. F., Introduction to Plasma Physics and Controlled Fusion Volume 1: Plasma Physics, Plenum Press, 1990.
- ¹⁸Divergilio, W.F. et al, "High Frequency Plasma Generators for Ion Thrusters," NASA CR-167957, November, 1981.
- ¹⁹Matsubara, Y. et al, "Development of Microwave Plasma Cathode for Ion Sources," Review of Scientific Instrument, Volume 61 Number 1, January 1990, pp. 541-543.
- ²⁰Satori, S. et al, "Operational Characteristics of Microwave Discharge Neutralizer," IEPC 97-031, 1997.
- ²¹Kuninaka, H., et. al., "Development and Demonstration of a Cathode-less Electron Cyclotron Resonance Ion Thruster," Journal of Propulsion and Power, Volume 14, Number 6, November-December 1998.
- ²²Kuninaka, H., et. al., "Result of 18,000-hour Endurance Test on Microwave Discharge Ion Thruster Engineering Model," AIAA 2000-3276.
- ²³Funaki, I., et. al., "Overdense Plasma Production in a Low-power Microwave Discharge Electron Source," Japan Journal of Applied Physics, Volume 40, 2001, pp. 2495-2500.
- ²⁴Kuninaka, H., et. al., "Development of 20 cm Diameter Microwave Discharge Ion Engine $\mu 20$," AIAA 2003-5011.
- ²⁵Kuninaka, H., et al., "Flight Report during Two Years on HAYABUSA Explorer Propelled by Microwave Discharge Ion Engines," AIAA 2005-3673.
- ²⁶Alton, G.D., and Liu, Y., "Future Prospects for ECR Plasma Generators with Improved Charge State Distributions," 28th Plasmadynamics and Lasers Conference, AIAA 97-2402, June 23-35, 1997.
- ²⁷Foster, J.E., et. al., "Discharge Characterization of 40 cm-Microwave ECR Ion Source and Neutralizer," AIAA Paper 2003 - 5012.
- ²⁸Kamhawi, H., Foster, J.E., and Patterson, M. J., "Operation of a Microwave Electron Cyclotron Resonance Cathode," 40th Joint Propulsion Conference, Fort Lauderdale, July 11-14, AIAA Paper 2004-3819.
- ²⁹Jasik, H., Editor, Antenna Engineering Handbook, McGraw Hill Book Company, New York, Chapter 9, 1961.

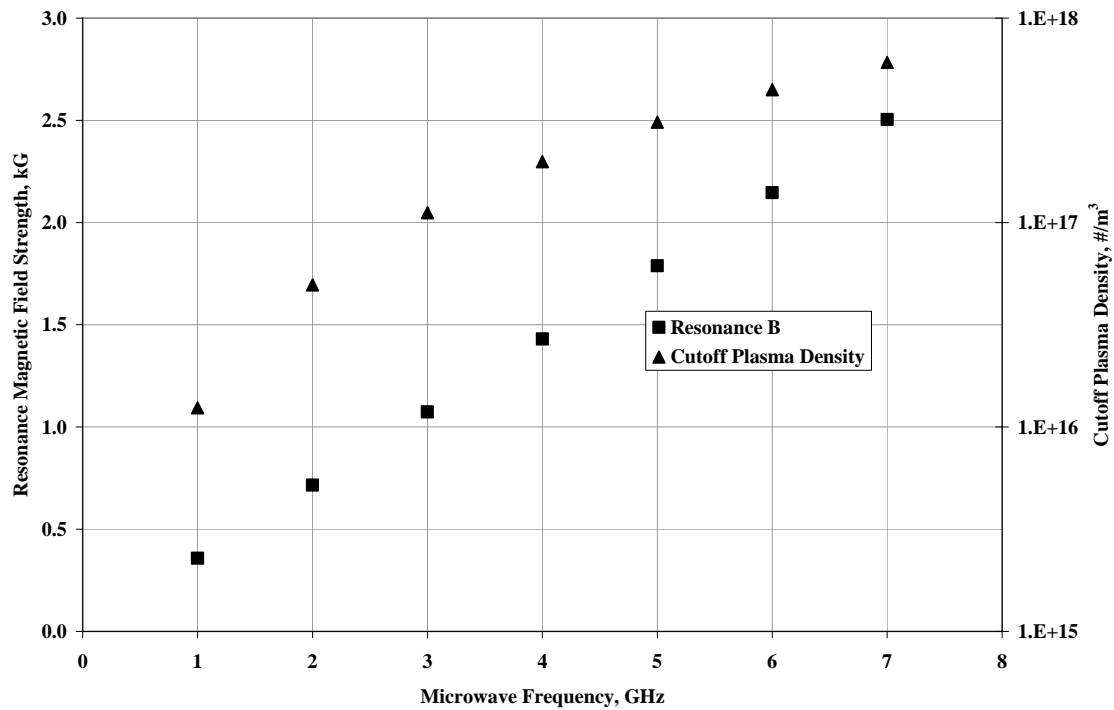


Figure 1. Calculated resonance magnetic field and cut-off density magnitudes for different μ wave frequencies (right hand Y-axis is a log scale).

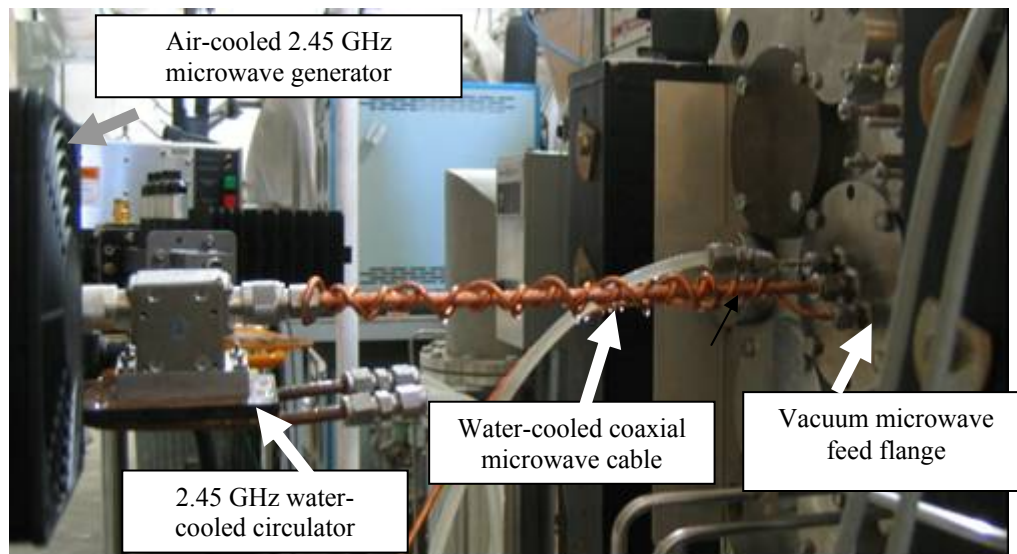


Figure 2. 2.45 GHz μ wave circuit.

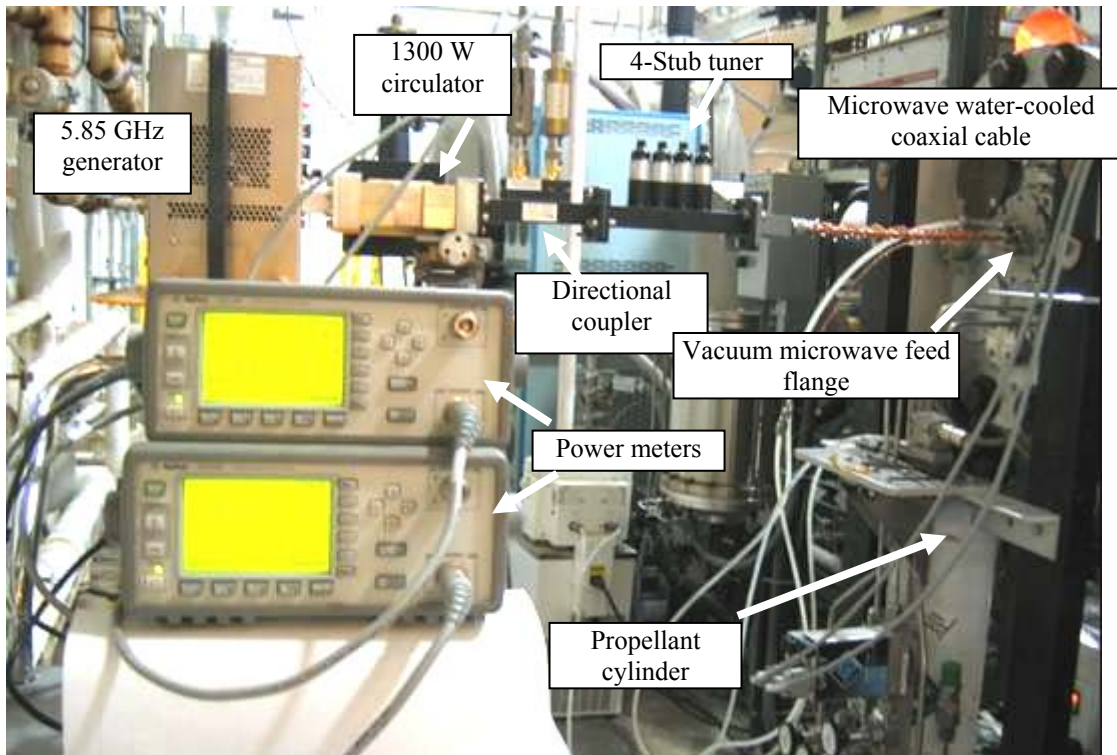


Figure 3. 5.85 GHz circuit with coaxial μ wave cable.

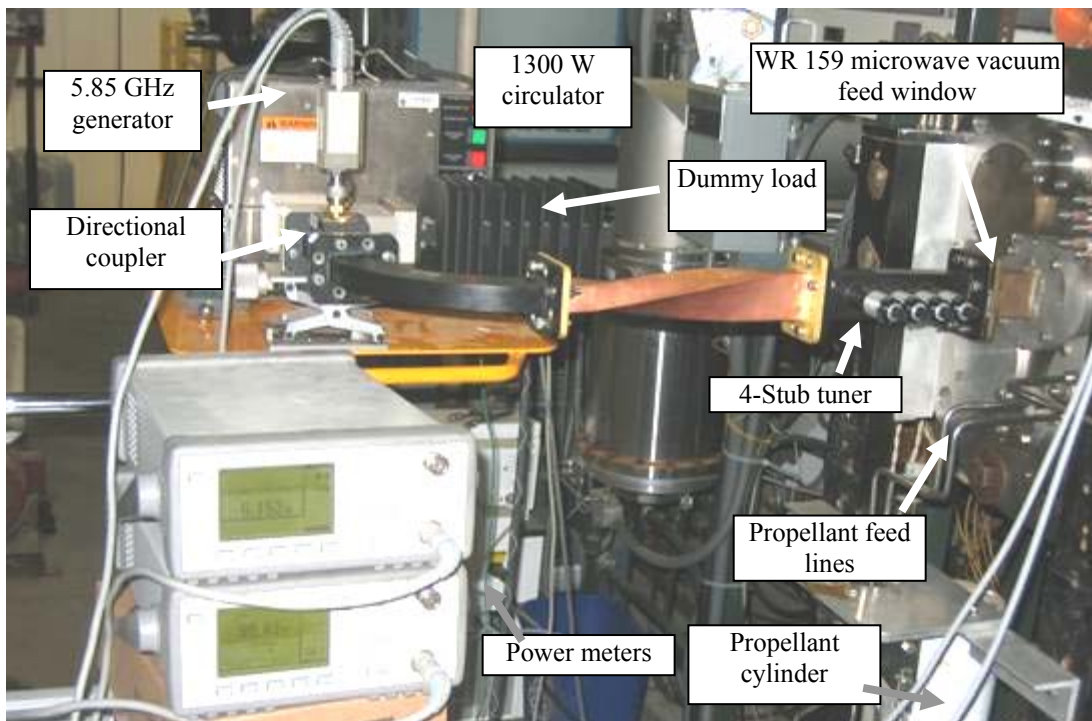


Figure 4. 5.85 GHz with waveguide μ wave circuit.

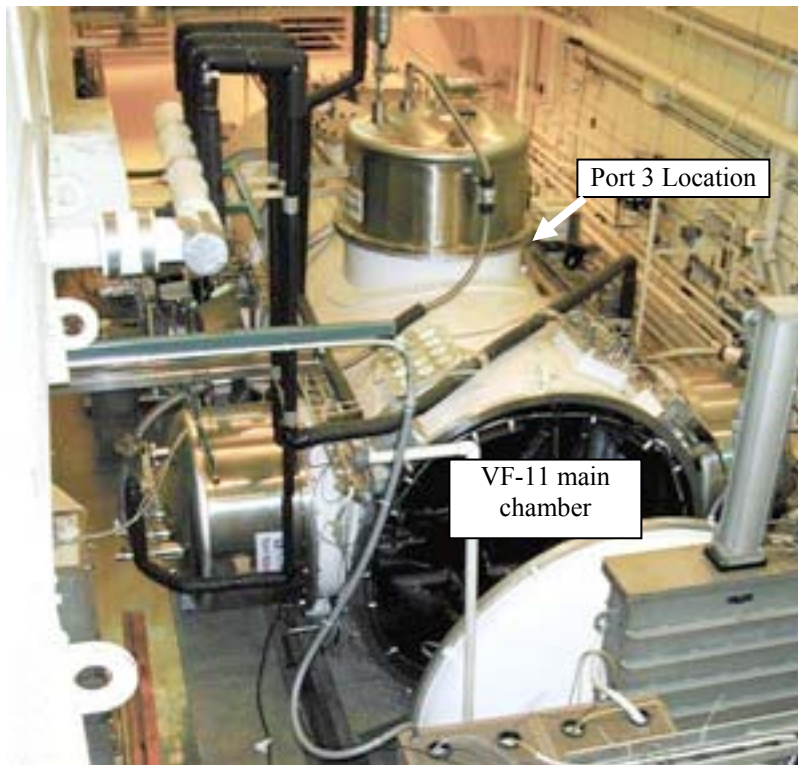


Figure 5. Vacuum Facility 11 and Port 3.

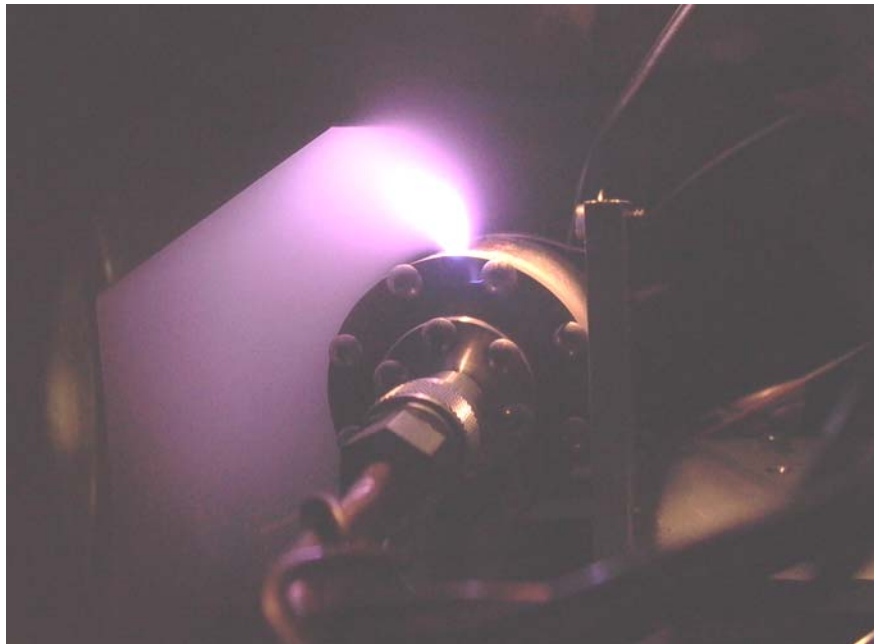


Figure 6. Configuration 1a ECR cathode operating at 100 W.

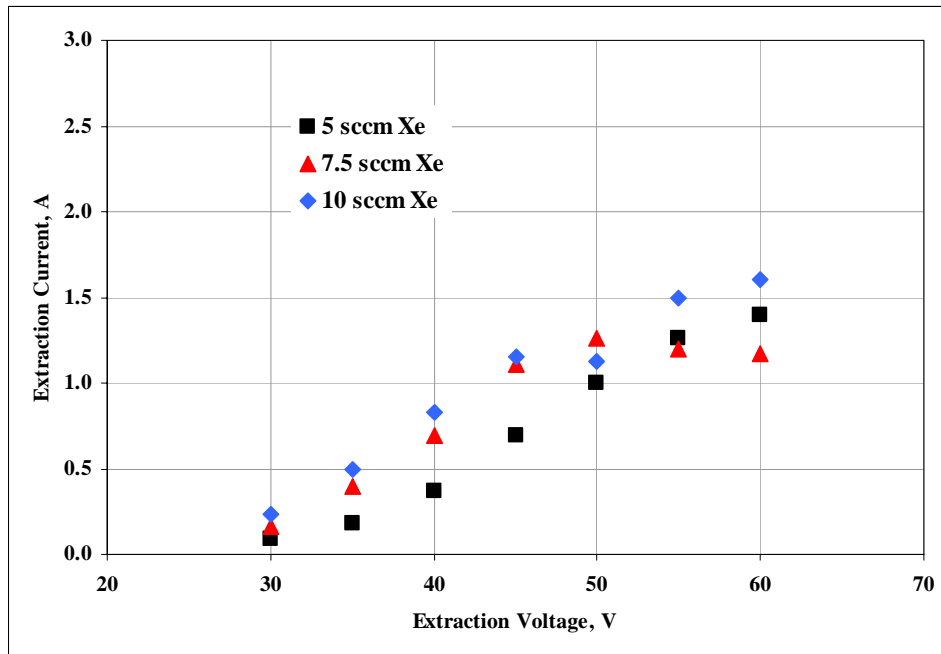


Figure 7. Electron extraction current magnitudes for Configuration 1a at 2.45 GHz and 75 W.

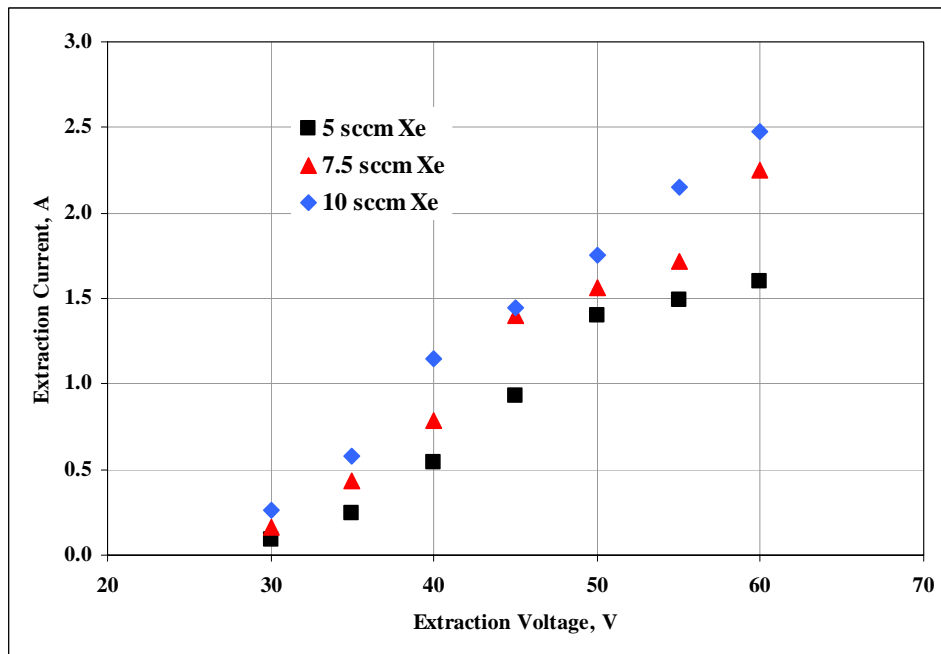


Figure 8. Electron extraction current magnitudes for Configuration 1a at 2.45 GHz and 100 W.

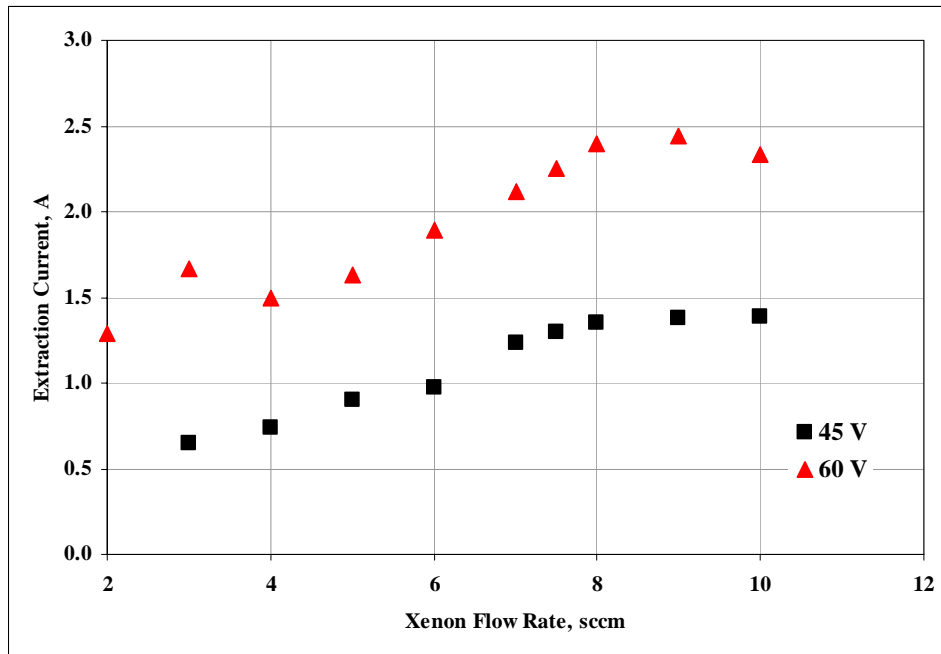


Figure 9. Variations in the electron extraction current magnitudes for extraction voltages of 45 and 60 V for Configuration 1a at 2.45 GHz and 100 W.

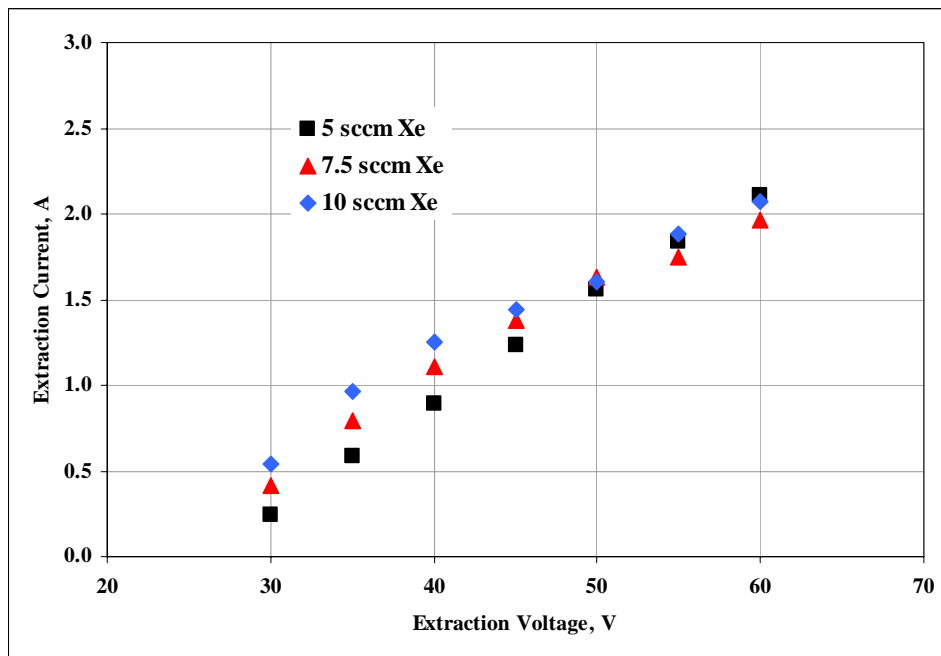


Figure 10. Electron extraction current magnitudes for Configuration 1b at 2.45 GHz and 75 W.

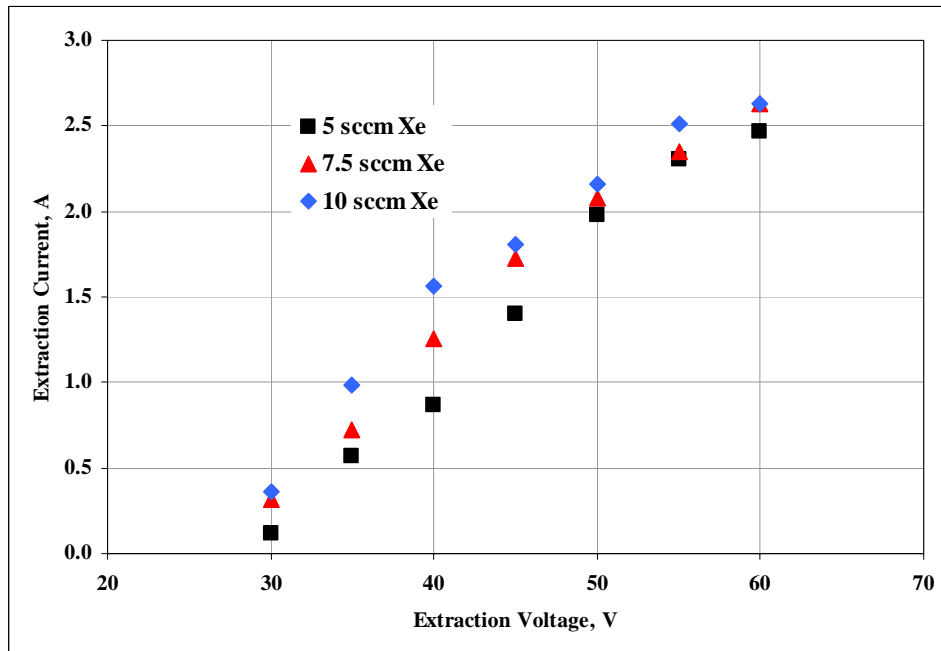


Figure 11. Electron extraction current magnitudes for Configuration 1b at 2.45 GHz and 100 W.

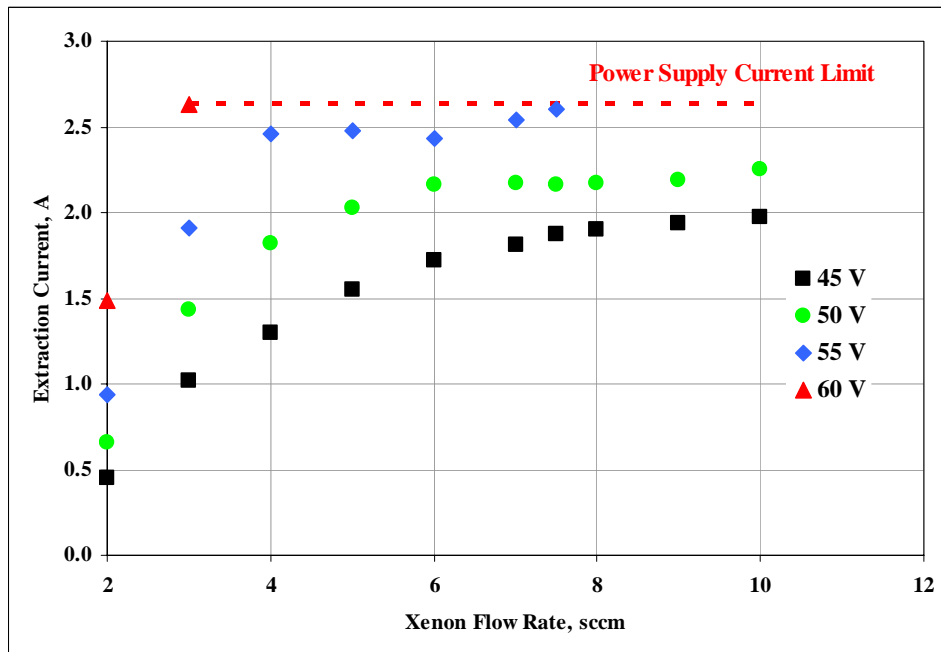


Figure 12. Variations in the electron extraction current magnitudes for extraction voltages of 45, 50, 55, and 60 V for Configuration 1b at 2.45 GHz and 100 W.

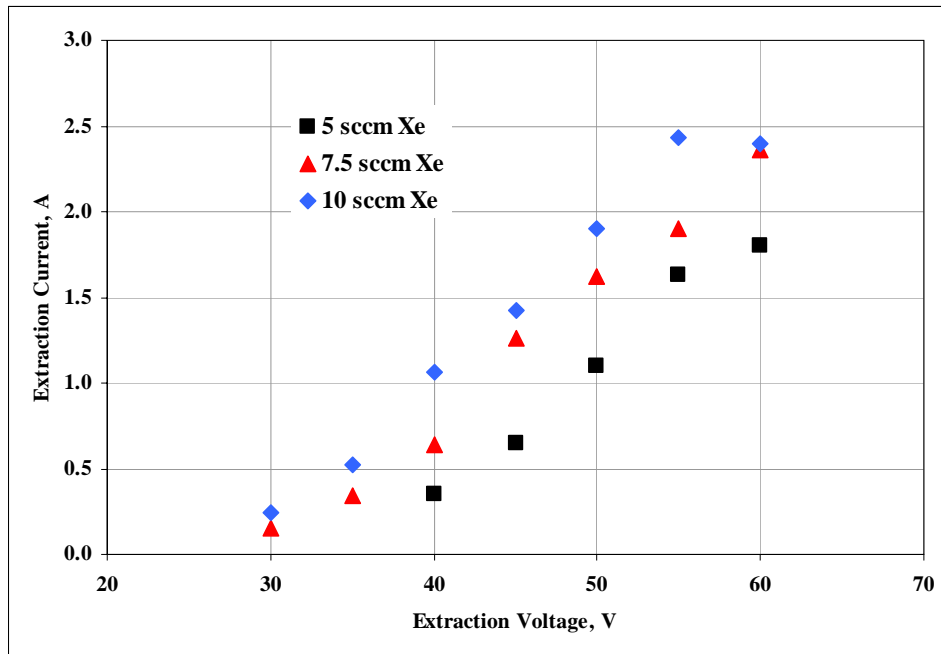


Figure 13. Electron extraction current magnitudes for Configuration 1a at 5.85 GHz and 100 W.

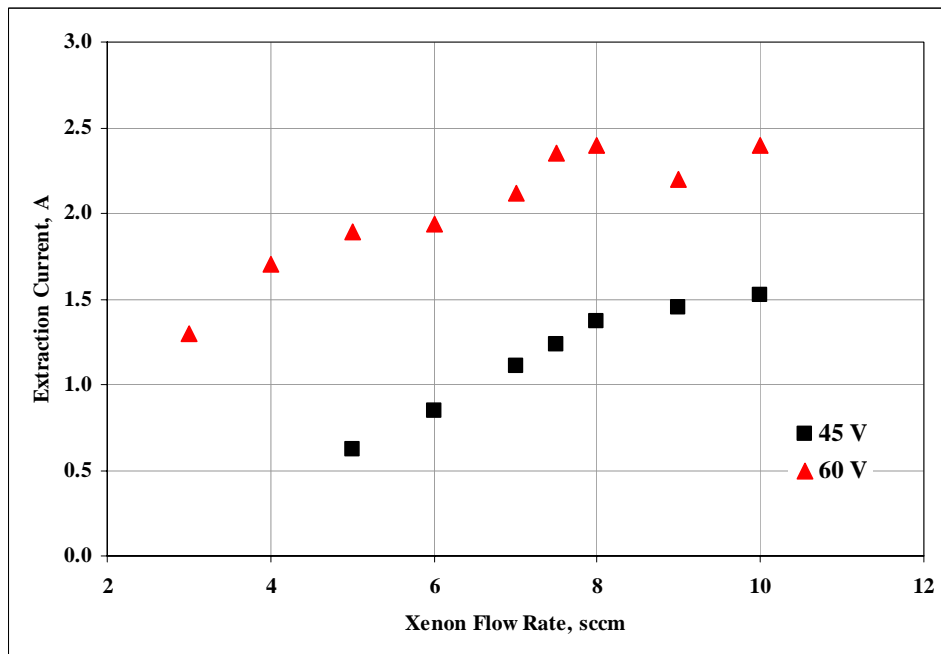


Figure 14. Variations in the electron extraction current magnitudes for extraction voltages of 45 and 60 V for Configuration 1a at 5.85 GHz and 100 W.

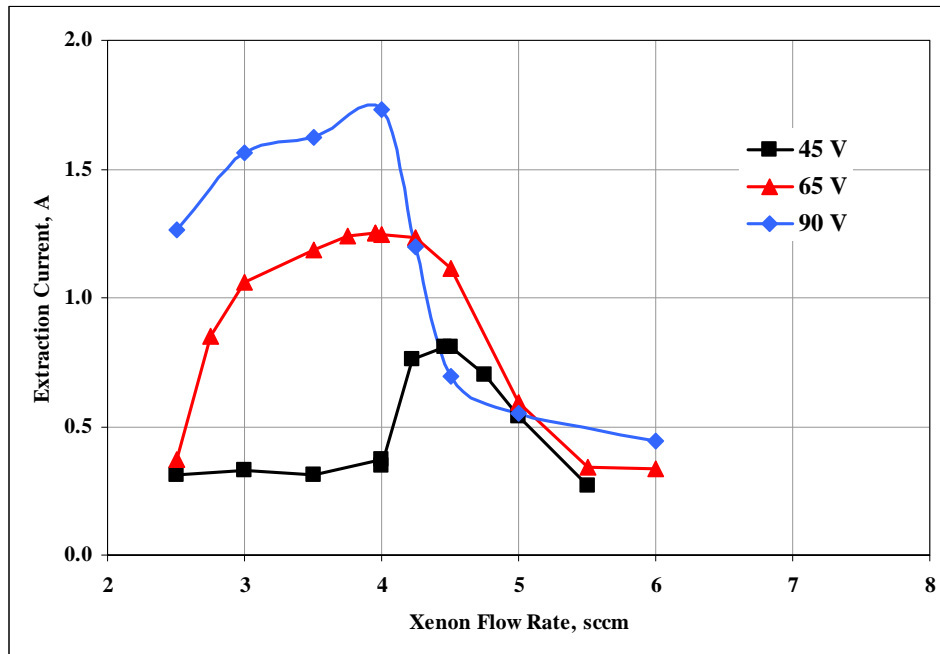


Figure 15. Variations in the electron extraction current magnitudes for extraction voltages of 45, 65, and 90V for Configuration 3a at 5.85 GHz and 100 W.

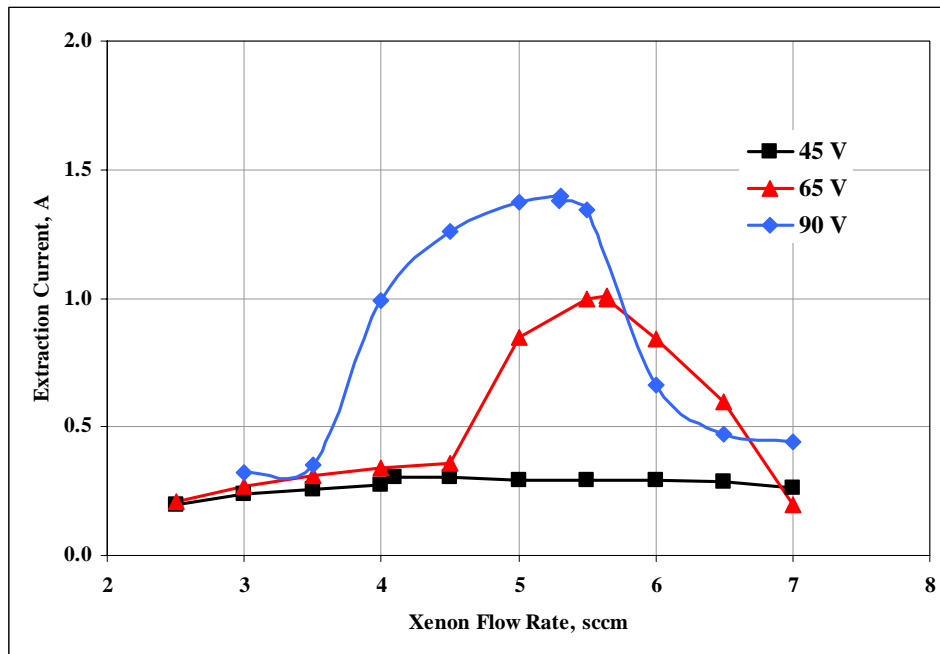


Figure 16. Variations in the electron extraction current magnitudes for extraction voltages of 45, 65, and 90V for Configuration 3b at 5.85 GHz and 100 W.